DNA at conductive interfaces: What can atomic force microscopy offer?

Kateryna Muzyka, Felix Rico, Guobao Xu, Ignacio Casuso

Journal of Electroanalytical Chemistry 938 (2023) 117448

Contents lists available at ScienceDirect

Journal of Electroanalytical Chemistry

journal homepage: www.elsevier.com/locate/jelechem

DNA at conductive interfaces: What can atomic force microscopy offer?

Kateryna Muzyka [a,b,*], Felix Rico [a], Guobao Xu [c,d], Ignacio Casuso [a,*]

[a] Aix-Marseille University, INSERM, CNRS, LAI, 13009 Marseille, France
[b] Kharkiv National University of Radio Electronics, Department of Biomedical Engineering, Laboratory of Analytical Optochemotronics, 61166 Kharkiv, Ukraine
[c] State Key Laboratory of Electroanalytical Chemistry, Changchun Institute of Applied Chemistry, Chinese Academy of Sciences, 5625 Renmin Street, Changchun, Jilin 130022, China
[d] University of Science and Technology of China, Hefei, 230026, China

ARTICLE INFO

Keywords:
Deoxyribonucleic acid
Electrode/electrolyte interface
Electrochemical sensors
Atomic force microscopy
Heterogeneity
Nanoscale

ABSTRACT

This review is devoted to the analysis of the capabilities of atomic force microscopy (AFM) in the study of the behavior of DNA at conducting solid–liquid and solid-air interfaces under electrochemical control and after the influence of the potential differences. The first part of the review presents the main aspects of AFM, the physical and chemical properties of DNA, and the behavior of DNA at conductive interfaces under the action of an electric field. The second part highlights the main categories of AFM applicability for DNA analysis at conducting interfaces from the point of view of "electrical stimulus-structure", "process-structure", and "process-structure-electrochemical properties" correlation. The applicability of AFM's main capabilities is shown: (i) visualization (of both monolayers and single molecules and hybridization complexes of DNA on a conductive surface), (ii) single-molecule force spectroscopy under electrochemical control, (iii) manipulation of DNA position at the nanoscale level. This review can be a starting point for further multidisciplinary DNA studies at electrochemical interfaces.

1. Introduction

Deoxyribonucleic acid (DNA), the carrier and transmitter of genetic information in biological systems, has fascinated biologists, chemists, and physicists. However, current interest in DNA goes beyond its role in biology. In recent decades, nucleic acid-based research is also related to investigating the behavior of DNA in different environments and under the influence of an external stimulus. In this context, the study of DNA behavior on conductive surfaces gains special attention, as it opens opportunities for elucidating the role of electric fields on the *fundamental properties of DNA*, such as electron transfer [1,2], electric field-induced DNA melting [3], electrochemical desorption of immobilized DNA probes [4–6], electrical potential-assisted DNA hybridization [7], conformation-dependent characteristics [8], oxidative DNA damage [9], electrically controlled DNA adhesion [10].

In turn, understanding of these characteristics may stimulate progress of DNA-based research in the areas of:

- biosensors (nucleic acid-based sensors) that use electrochemical [9,11] and electrochemiluminescent [12,13] signal transduction;
- material science (as a novel functional material based on DNA interfaces with dimensional materials [14])
- bioelectronics [15], etc.

The above-cited works have provided indirect evidence that the nature of DNA distribution on the conductive surface affects the conformation/orientation, the steric interaction, the steric and electrostatic barriers to hybridization, the melting temperature and the sensitivity to electric fields, the sensing properties of the DNA layer, etc. Therefore, in line with the investigation of DNA behavior at the conductive solid/liquid interfaces under the influence of the electrical field, understanding the "structure-functional behavior" correlation of DNA on electrodes is a prerequisite for overcoming the scientific and technological difficulties that inhibit the transition from fundamental studies to practical applications and from proofs-of-concept to the commercial application of DNA-based electrochemical platforms.

DNA characterization methods at the conductive interface, in particular, electrochemical methods, provide information about the entire surface. The influence of surface heterogeneity at the nano level on the system's overall behavior remains underestimated. Hence, there is limited understanding of the relationship between the character of DNA distribution on the electrochemical surface with the functional properties of such interfaces, which may drive to non-reproducible results. Therefore, nanocharacterization methods of DNA at the electrochemical interface are an essential addition to the current approaches of characterization at larger length scales.

* Corresponding authors at: Aix-Marseille University, INSERM, CNRS, LAI, 13009 Marseille, France (K. Muzyka).
E-mail addresses: kateryna.muzyka@nure.ua (K. Muzyka), ignacio.casuso@inserm.fr (I. Casuso).

https://doi.org/10.1016/j.jelechem.2023.117448
Received 31 January 2023; Received in revised form 26 March 2023; Accepted 9 April 2023
Available online 11 April 2023

Scanning probe based microscopy methods, in particular, atomic force microscopy (AFM) with its unique capability to perform high-resolution imaging and characterize organic and inorganic samples at ambient pressure under air, liquid, and vacuum conditions [16], are valuable tools for understanding the complex architecture of nanoscale structures and for studying microscopic and submicroscopic objects below the diffraction limit of optical microscopy. Moreover, the power of AFM and related techniques can go beyond static topography images. Uniquely valuable tools are, for example, force spectroscopy, to characterize physico-chemical surface properties [17] and high-speed AFM (HS-AFM) to observe dynamic features [18]. DNA has been imaged by AFM, with increasing success, for more than 20 years [19], and reviews on the progress of DNA imaging by AFM, from early images of DNA in air to high-resolution mapping in fluid, have been recently [20]. Moreover, with the development of HS-AFM, it is becoming possible to observe directly DNA-protein interactions and dynamics with relevant spatial and subsecond temporal resolutions [21].

Despite of the fact that the imaging of single DNA strands immobilized on mica (which is a dielectric) by AFM has become routine [22–24], much of what was learned about the nanoscale conformations of adsorbed DNA on mica may not automatically translate to DNA adsorbed on conducting supports, such as gold or carbon-based materials; which are frequently used as an electrode of electrochemical biosensor [25,26]. Therefore, additional studies will be needed that will assess the capabilities of AFM to investigate DNA on surfaces other than mica. That can open possibilities to nanoscale investigation of DNA at conductive surfaces in presence of electric fields.

Here, we provide an overview of recent advances on AFM-based probing of DNA at conductive interfaces, shedding light on the current understanding of the behavior of such interfaces at the nanoscale, and providing an outlook on the most-promising AFM capabilities in this context. To better understand the applicability of AFM in the characterization of DNA on conductive solid/liquid interfaces and to evaluate the prospects of this direction, we briefly introduce the reader to the essential physicochemical properties of DNA, summarizing them in the appropriate subsections. In addition, to acquaint the untrained reader with the potential possibilities of AFM, we provide brief information about the basic modes of operation of AFM for the study of biological samples, as well as highlight the advantages and limitations of these methods.

2. Background theory

2.1. The basis of AFM

AFM is a very high-resolution scanning probe microscopy with demonstrated resolution on the order of fractions of a nanometer, more than 1000 times better than the optical diffraction limit. Moreover, AFM operated under vacuum or ultrahigh vacuum is capable of resolving atomic scale features. In general terms, AFM provides nanoscale information of the roughness, physico-chemistry and topography of the surface. It can map the surface architecture, homogeneity, and distribution of biological receptors immobilized on solid supports in the air or under fluid. AFM can yield topographical images of conducting and nonconducting samples in almost any environment without using costly and time-consuming sample preparation techniques. It does not require freezing, drying, tagging the sample with dyes, or using metal coating on the sample like, for example, electron microscopy. Basic information on imaging and force spectroscopy modes of AFM of biological samples is summarized in Table 1.

The most essential component of AFM is a nanoscale tip (typically $<$ 50 nm in diameter) that is attached to a small cantilever which, in first approximation, can be modeled as a spring. The cantilever tip (AFM probe) interacts with the substrate while it performs a raster scanning motion that follows the sample surface corrugation at molecular scale. The vertical and lateral movement of the AFM probe (deflection of the cantilever) monitors the tip-sample interaction forces. Registration of the cantilever deflection is carried out using an optical system, in which a laser beam is focused on a reflective coating on the back of the cantilever, reflecting onto a position-sensitive detector (PSD) or split photodiode. The deflection of the cantilever (nanometers of displacement) causes corresponding changes in the position of the laser beam reflected from the back of the cantilever on the PSD. Thus, the shifting of the laser beam on the photodetector corresponds to a voltage change that is converted in to deflection and then force, upon calibration of the system. The cantilever signal is used by a feedback system to maintain a constant interaction with the surface upon scanning. A conventional AFM can image a maximum height on the order of 10–20 μm and a maximum scanning area of about 150 × 150 μm [27]. **The spatial resolution** of AFM largely depends on the cantilever tip and the sample properties. The typical ***lateral resolution*** of AFM: (~20 nm) due to the convolution. For sharp tips: 2–3 nm in the lateral direction (sub-molecular resolution for proteins) [28]. The ***vertical resolution*** is mainly limited by the thermal noise of the deflection detection system. Most commercial AFM instruments can reach a vertical resolution as low as 0.01 nm for more rigid cantilevers. However, one should bear in mind the deformation of the tip and sample, which may be significant-particularly for soft materials such as biological samples. Therefore, softer samples, such as cells, limit importantly the values of resolution.

There are two basic modes of imaging surface topography with an AFM: Static or Contact mode, and dynamic (tapping) mode AFM. Tapping mode is generally more applicable to the non-destructive imaging of “soft” or biological interfaces, as the lateral forces are reduced, preventing the tip and sample from getting damaged.

Although the AFM is primarily an imaging tool, it also allows measurement of inter- and intramolecular interaction forces with piconewton resolution [29]. In AFM “force spectroscopy” experiments, the cantilever and tip are moved directly towards the sample until contact is made, and then retracted again, while the interaction between the tip and sample is measured [30].

2.2. The physico-chemical features of DNA at electrode/electrolyte interface

In discussing DNA on conductive surfaces, it is necessary to mention the nature of the electrode/electrolyte interface. Any interface will influence the electrolyte solution since the interactions between the solid and the electrolyte will differ considerably from those in the solution. For electrodes under potentiostatic control, there will also be an additional influence on the charge held at the electrode. These factors result in strong interactions between the ions/molecules in the solution and the electrode surface. This gives rise to a region called the electrical double layer. Many models have been developed to explain the behavior observed when electrochemical measurements are performed in electrolyte solutions [38].

For conducting an AFM experiment on the study of DNA at a solid–liquid interface, it is necessary to have an idea of the factors that can affect the behavior of DNA and, therefore, will facilitate the interpretation of the results. In Table 2, we briefly present the main features of the solid–liquid interface.

In Table 3, we summarized essential information on the physical chemical properties of DNA that can be a starting point for a deeper understanding of aspects related to the subject of this review.

The DNA susceptibility to the electric field in the EDL of electrode/-electrolyte interface is caused by (i) the presence the highly negatively charged sugar-phosphate backbone at neutral pH and (ii) location the hydration shell of DNA and its condensed counter ions which can occupy a significant portion of the diffuse part of the EDL [8].

Table 1
Basic information on imaging and force spectroscopy modes of AFM of biological samples.

STATIC MODE (CONTACT MODE**)** [31,32]
Main principle. The tip's force applied to the sample is kept constant. The lowest force measured by AFM is in the order of one pN (see Ref. [16]). AFM can measure the cantilever deflection down to 0.1 nm. Contact mode allows friction maps. **Feedback signal**: cantilever deflection. **Spring constants of cantilevers:** low of < 0.1 N/m **A typical scan rate:** 1 line/s. For high-speed scanning: 100 line/s). **Force. Mainly repulsive forces,** >10 pN (depending on the sample) **Feedback signal.** Cantilever deflection or force. **Main disadvantages.** • Generation of lateral forces during scanning that may deform, displace or damage soft biological samples. • High-resolution imaging requires that the samples are well immobilized, e.g., by adsorbing DNA at very high concentration on cationic surfactant bilayers.
DYNAMIC MODE (TAPPING MODE) **and MECHANICAL MAPPING**[32–37]
Main principle. The cantilever is oscillated close to the sample surface; tip-surface interactions change the cantilever oscillation amplitude and/or resonance frequency. The oscillation amplitudes are approximately 5–100 nm. (Note: it can be reduced to 100 pm or less, if tuning forks are taken into account). *Two resonant modes*: First, the operation is near the resonance frequency of the cantilever. Second, at a frequency low enough to be out of the cantilever's resonance frequency (off-resonance modes). The off-resonance modes are optimal for measuring the mechanical properties of the samples, they are also termed mechanical mapping. **Spring constants of cantilevers:** 0.1–50 N/m **Feedback signal.** Cantilever oscillation amplidue (>5 nm) or frequency **A typical scan rate (The data acquisition (sampling) rate):** 1 line/s. For high-speed scanning: 100 line/s. **Force.** Both repulsive and attractive forces **Obtaining topography data**. By measuring amplitude variations and terminating the z feedback loop to compensate for these changes. **Obtaining mechanical data**. By analyzing the deflection of the cantilever during the interaction with the sample (off-resonance). **The main disadvantages**. The sample's structural, mechanical, and chemical properties can affect the cantilever amplitude that complicates topographic data interpretation. The factors affect the resolution of the tapping mode AFM imaging in fluid [20] via the effects of fluid damping, and the convolution of the cantilever resonance with the mechanical resonances of the fluid cell (“forest of peaks”)
AFM FORCE SPECTROSCOPY and FORCE MAPPING [17,29,30]
Main principle. The cantilever is approached and retracted from the sample surface while the interaction is monitored. This allows determination of mechanical or physico-chemical properties of the sample. **Force range (pN):** 10–10^4. **Spring constants of cantilevers:** 0.01–10^5N/m **A typical speed of the tip**: 1 μm/s. **The maximum approach speed:** <10 μm/s (for conventional cantilevers and instruments); ~10 mm/s (in recent HS-AFMs) [17]. **The maximum retraction speed:** ~10 mm/s (for an advanced high-speed AFM) [17]. Force mapping implies obtaining force spectroscopy measurements at different locations across the sample surface.

Table 2
The main features of the solid–liquid interface.

A solid–liquid interface
When an solid conductor is brought in contact with a liquid ionic conductor (electrolyte), a common boundary (interface) between the two phases appears. Both electron transfer and ion transfer co-exist at the solid–liquid interface.
Electrical double layer, EDL
For solid conductors in the electrolyte under potential: • Interaction of the atoms/molecules in the solution with the atoms on the conductive surface leads to form an overlap of electron clouds. • Electron transfer occurs first to make atoms on the solid surface charged, i.e., the formation of ions. • Due to electrostatic interactions, ions in the liquid migrate toward the surface bonded ions, forming an EDL.
Structure of the Electrical double layer, EDL (according to Stern):
• STERN LAYER is fixed to the solid surface. It has positive or negative ions. There is a sharp fall in potential. • DIFFUSE LAYER extends some distance into the liquid phase and is composed of ions attracted to the surface charge via the Coulomb force, electrically screening the first layer. The potential drops off exponentially through the diffuse layer, approaching zero at the imaginary boundary of the double layer.
Electric surface charge of EDL
• Expresses in C/m^2 and creates an electrostatic field that affects the ions in the bulk of the liquid. • The EDL charging time (τ) depends on the solution resistance and the electrode capacitance (τ = RC).
Zeta potential (ζ-potential)
• The ζ-potential is used for estimating the degree of EDL charge. • A characteristic value of zeta potential in the EDL is 25 mV with a maximum value of around 100 mV (up to several volts on electrodes). • The point of zero charges (the ζ-potential is 0) is called the *isoelectric point.*
Debye length
• The Debye length is the characteristic thickness of the EDL. It is reciprocally proportional to the square root of the ion concentration (with increasing concentration, the thickness of Debye length decreases). • Typical scale of Debye length in aqueous solutions: a few nanometers. • Electric field strength inside the EDL: from zero to over 10^9 V/m.

Table 3
The basic physical–chemical properties of DNA.

Chemical structure of DNA [41]
• DNA is a linear, oligomer-like chain of nucleotides. Composed of a ribose sugar, a phosphate group, and an attached nitrogenous heterocyclic base. • DNA and ribonucleic acid (RNA) are nucleic acids.
• Aptamers are short sequences of artificial DNA, RNA. • The nucleotide units build up single-stranded (ss) DNA and are connected via oxygen atoms. • Most DNA molecules are two polymer strands bound together in a helical fashion by noncovalent bonds forming a double-stranded (dsDNA) structure. structure. • Hybridization of two ssDNA occurs through specific base pairing: *adenine (A) – thymine (T)* or *guanine (G) – cytosine (C)* via hydrogen bonds, resulting in a helical structure form of the double-stranded (ds)DNA.
• During melting, the two strands can come apart to form two ssDNA.
Contour length (Lc) of DNA
• The *contour length* (*Lc*) of a polymer chain (a large molecule consisting of many similar smaller molecules) is its length at the maximum physically possible extension. The contour length is equal to the product of the number of segments of polymer molecule (*n*) and its length (*l*). • in DNA sensors, the typical *Lc* is of 5–10 nm (equal to 16 to 30 nucleobases).
Inter-base and end-to-end distances of DNA [48]
• 0.64 nm is the distance between bases for an ssDNA with a small and identical number of bases. • 0.34 nm inter-base distance for dsDNA. • ssDNA with more bases yields shorter *end-to-end distances* than dsDNA because it curls over on itself much more on average, reflecting its shorter persistence length.
The persistence length (Lp) and flexibility [48–52]
• The "mechanical" *persistence length* (*Lp*) is defined as "the length over which the tangent vectors at different locations on the chain are correlated" is 1–2 nm for ssDNA and 50 nm for dsDNA. • *Lp*, the effective *persistence length*, is a sum of the intrinsic stiffness, the persistence length of the molecule (*Pi*) and an electrostatic persistence length (*Pe*) which depends on the ionic strength [53]: $Lp = Pi + Pe$. • At low ionic strength, electrostatic self-repulsion in the phosphate backbone (*Pe*) prevails, thus tends to increase effective *Lp*, but at high salt concentrations, dominates the intrinsic rigidity of the phosphate backbone (*Pi*) and thus tends to increase effective *Lp*.
• The flexibility of DNA depends on the ionic strength of the electrolyte solution. • For ssDNA lengths with $>$ 150 bases, the ssDNA chain is considered a flexible polymer. • For short dsDNA ($Lp \sim 50$ nm), the ds DNA is considered rigid and rod-like ($Lc < Lp$) (in environments containing salt concentrations greater than ten mM).
• Lp of the capture probe is changed upon hybridization. • The local ssDNA bending and chain twisting is also sequence-dependent. • AFM is a powerful technique to study DNA flexibility, either by imaging or force-spectroscopy approaches.
Acidic properties and charge [54]
• DNA is similar to phosphoric acid due to the phosphate groups and behaves as a strong acid. • DNA is fully ionized at a normal cellular pH, releasing protons that leave behind negative charges on the phosphate groups. Negative charges protect DNA from breakdown via hydrolysis by repelling nucleophiles which could hydrolyze it.
Stability [55–58]
• DNA is chemically relatively stable, which makes it easy to handle. • Long-term storage of the primary and secondary structure of DNA is possible at room temperature under conditions of protection from water and oxygen [55]. • Upon dehydration (between 92% and 70% relative humidity), DNA undergoes conformational changes from form B to form A.
• Below 70–50% RH at room temperature, natural DNA undergoes denaturation. • DNA samples are usually stored at -20 °C, but freezing can alter the structural integrity of the DNA molecules.

Numerous experimental studies [39–43] of surface-tethered single- and double-stranded DNA at the electrode/electrolyte interface reveal the following results:

i. *A strong field within the EDL layer is sufficient to induce a distinct conformational state of DNA.*
   - the Gouy-Chapman model (adopting a salt concentration of 60 mM and a surface potential of 0.2 V) predicts an electric field strength of 160 kV/cm at the surface. In contrast, its magnitude has decreased to 0.5 kV/cm at 9.2 nm, which corresponds to the DNA's top end when "standing" on typical DNA biosensor surfaces.

The gradient of the electric field calculated according to the Gouy–Chapman model is shown in Fig. 1, left.

- For electrolyte concentration larger than 100 mM (NaCl), the ability of the electrode field to orient dsDNA (24 and 48 base pairs) at the electrode is lost.

ii. *The electrically induced motion of DNA at the electrode/electrolyte interface is correlated to the characteristic charging time (τ) of the EDL,* e.g., via the variation of the ionic strength of the solution and the size of electrode.

iii. *The short-ranged electric field governs only a few DNA segments closest to the surface and thus determines the equilibrium conformations for repulsive and attractive surface fields and the dynamic transitions between them.*

- Since the persistent length (L_P) of dsDNA (50 nm) is much higher than the Debye screening length (19 nm), only the charges that are within the Debye length will be effectively repelled when the electrode is negatively charged [10,45].

iv. *The stiffness of the DNA largely determines its dynamic behavior on the surface; for instance:*

- The switching behavior of ssDNA differs from dsDNA [44]. In the first case, the molecules are flexible due to their short L_P. As a result, only the lower part of the flexible ssDNA is stabilized by

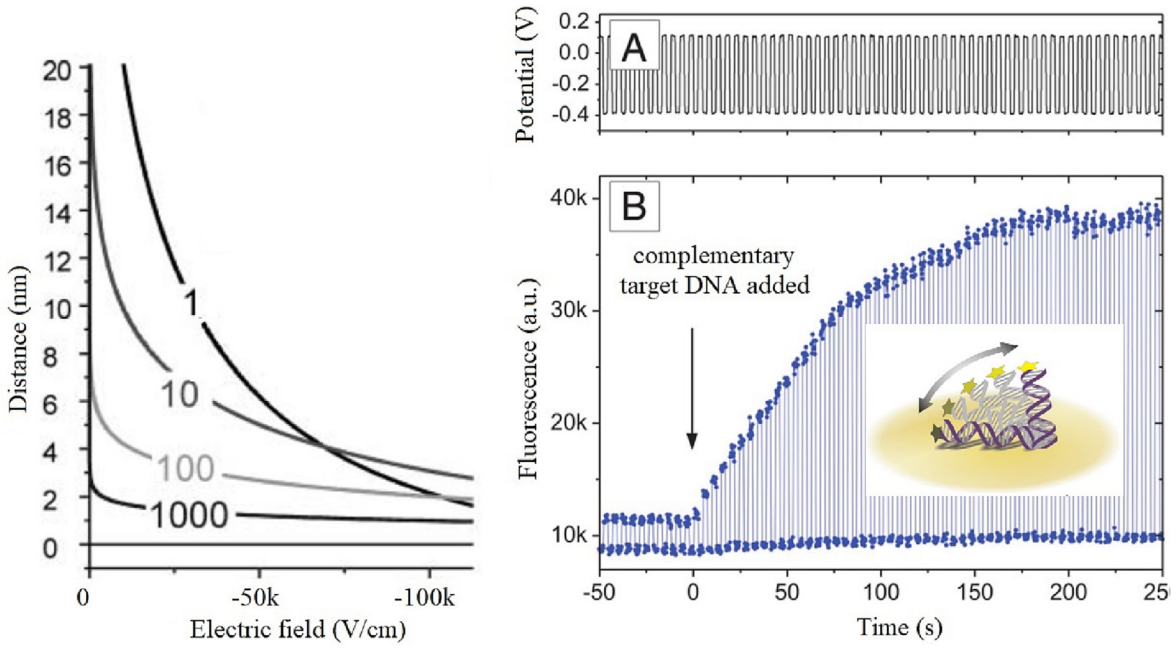

Fig. 1. Left. Electric field within the electrode surface, calculated using Gouy–Chapman approach for different concentrations of monovalent salt (numbers denote the concentrations in mM) and an electrode potential of −0.1 V (Adapted from Ref. [39] with permission). Insertion: ss- and dsDNA conformation depends on the electrode potential [45]. Right. (A) The potential applied to a gold electrode (vs. a Pt reference) that supports a layer comprised of 48-mer DNA of a mixed, nonself-complementary sequence. (B) The fluorescence emission of the Cy3-labeled DNA's upper ends (Insertion B). High FL intensity corresponds to upright DNA conformation. In contrast, low FL intensity to tilted conformation, as nonradiative energy transfer to surface plasmons in the metal substrate (e.g., gold), suppresses the FL of the dyes approach the surface. The arrow marks the injection of 100 nM fully complementary targets that hybridize with the initial ssDNA layer (Adapted from Ref. [44]).

the short-ranged repulsive field; the upper part is significantly coiled up (adopts a random configuration) (see Fig. 1, Left insertion).

- Rigid dsDNA, on the contrary, may be oriented efficiently by the electric torque acting on their lower parts, which aligns the molecule's upper parts due to the intrinsic stiffness of the helix.

v. *The dissimilar dynamic behavior observed for ss- and dsDNA can be related to their distinct flexibilities.*

- dsDNA responds to higher switching frequencies (from repulsive to attractive surface potentials) than ssDNA.

Thus, it is possible to discriminate dsDNA from ssDNA when modulated at high frequencies according to the individual kinetic "fingerprint" of switching dynamics [44].

- At high frequencies ($> \approx 10$ kHz), the DNA layer ceases to follow the electrical excitation. The DNA strands take an average position on the surface between a lying and a vertical orientation.
- At frequencies too high for the EDL to accumulate, electrostatic interactions with the surface are negligible, and thermal fluctuations govern the DNA's orientation. As a consequence, manipulation of the layer conformation is not feasible.

Taken together, the conditions mentioned above indicate why dsDNA layers can be switched more effectively than ssDNA layers. The representative switching experiments with end-tethered oligonucleotides illustrates the hybridization effect is depicted at Fig. 1, right. A low-frequency (0.2 Hz) square wave AC bias is applied to the gold electrode (Fig. 1, Right A), while the fluorescence (FL) emitted by the Cy3-labeled DNA layer is observed simultaneously (Fig. 1, Right B). Within each switching cycle, levels of high FL intensity correspond to negative substrate potentials, whereas low intensities correspond to positive bias. Here, the terms negative and positive are used with respect to the potential-of-zero charge, which is at approximately −0.2 V vs. Pt reference or 0.0 V vs. Ag/AgCl reference, respectively. At t = 0, the hybridization of the layer is initiated by adding an excess concentration (100 nM) of unlabeled complementary 48-nt targets to the solution capping the probe-DNA layer (Fig. 1, Right B). The binding of targets to the probe layer results in a marked and immediate increase in the measured switching amplitude; after the transformation from a single- to double-stranded layer is completed, the switching amplitude is enhanced by roughly one order of magnitude (in other measurements, enhancement factors > 25 were observed).

vi. *To realize the rotational freedom necessary for electrically switching DNA, neighboring DNA strands should not interact with each other causing steric hindrance.*

- No steric interactions between individual molecules are assumed to occur when the average spacing between two neighboring DNA strands is two times larger than the contour length of DNA [46].
- The inter probe interactions become significant when the probes are separated by <10 nm [47].
- Low molecule surface densities (<molecules 10^{11} cm^{-2}) are a prerequisite for the rotational freedom of DNA.
- In diluted samples, 24–48 bp long dsDNA monolayers on gold ($\Gamma_{DNA} \sim 5 \times 10^{11}$ molecules cm^{-2}) possess considerable rotational freedom, and the tilt angle of the double helix at positive potentials can be significant (70° vs. surface normal) [39].
- In more compact DNA monolayers ($\Gamma_{DNA} > 1 \times 10^{12}$ molecules cm^{-2}), the rotational freedom of DNA molecules is significantly restricted, and a large inclination of the double helix toward the Au surface (as an example) is impossible [39].

3. What can AFM offer in the investigation of DNA at electrified interfaces?

3.1. AFM imaging of DNA

3.1.1. Height based AFM – imaging of electrically induced changes of the DNA layers morphology

The phenomenon of a dramatic morphology change of DNA when bound to electrodes as a function of the electrode potential was first demonstrated in 1998 by Kelley et al. They used electrochemical atomic force microscopy (EC-AFM) to monitor the height of thiol-derivatized 15-base- pair DNA duplexes monolayer on Au(1 1 1) [59] (see Fig. 2).

The height measurement of the DNA films was carried out by the mechanical removal (scratching) of a small patch of DNA from (see Fig. 2 right insertion) the gold by applying a high vertical force with the AFM tip.

The procedure was as follows: decreasing the scan size to ~ 100–150 nm, increasing the scan rate to 24–30 Hz, and applying high vertical force by advancing the set point several units for 1 min. A slight hysteresis (~10-30-mV shift) in the film-height change was noticed when scanning the potential in the negative direction (see Fig. 2. Right). The slight negative charge of the Si_3N_4 probe tip in an aqueous solution at pH 7 was considered a possible reason for this hysteresis. However, most likely, in comparison with the total applied vertical force, surface/tip interaction was relatively small and may not alter the surface topography.

When applying potentials (versus an Ag wire quasi-reference electrode (QRE)) the DNA monolayer changed its morphology as shown in Fig. 2. These results are consistent with the Coulombic interaction between negatively charged DNA helices and the surface of working electrode under positive potential [60].

Employing EC-AFM, it was possible to characterize a ~4 nm variance in DNA-film thickness applying only minor changes in the applied electrochemical potential (~75 mV). Thus, high sensitivity DNA to the surface charge opens the way for the preferred helical orientation in a controlled manner by using slight electrical potential difference. Moreover, such changes in morphology are reversible. Although the film is very stable under open-circuit conditions, application of either large positive or negative potentials ($-0.5\ V \leq E_{app} \leq 1\ V$ versus Ag wire) result in rapid desorption of the monolayer, owing to redox reactions that occur at the gold-thiol linkages.

Even though the visualization of individual DNA molecules under the influence of an electric field have not been reached, this study demonstrates that by applying a positive potential it is possible to regulate the strength of the interaction of DNA molecules with the surface, thus opening the possibility of achieving high-resolution AFM imaging in situ by selecting appropriate potentials.

3.1.2. AFM topographic imaging of the nucleic acid-based electrochemical biosensor surface

The International Union of Pure and Applied Chemistry (IUPAC) defines an electrochemical nucleic acid-based biosensor as a device that incorporates nucleic acids as a biological recognition element and an electrode as a physicochemical transducer. The applications of DNA electrochemical biosensors are based on the interaction of the analyte of interest with the DNA detection layer immobilized onto the electrode. The DNA-analyte interaction at the nanoscale causes changes in the DNA structure, morphology, and electrochemical behavior [9]. The interactions of DNA with solid electrode surfaces are a significant concern in DNA electrochemical biosensor development, as the adsorption characteristics of DNA is crucial for biosensor performance in terms of reproducibility and reliability.

A series of intensive studies using Magnetic AC mode (MAC mode) AFM have been undertaken by the group of Oliveira-Brett [61–66] to characterize the morphology of a nucleic acid-based electrochemical biosensor.

Below we have outlooked two prominent examples of MAC Mode AFM characterization (in the air condition) of nucleic acids adsorbed onto a highly oriented pyrolytic graphite (HOPG) electrode under applied potentials, described in Refs. [66] and [61], respectively. In both studies have been used a MAC Mode AFM characterization in air conditions with type II MAC levers of 225 μm length, tip radius of curvature less than 10 nm, 2.8 N/m spring constant, and 60–90 kHz resonant frequencies, with scan rates of 1.0–2.5 lines s^{-1}.

3.1.2.1. AFM characterization of oligodeoxynucleotides adsorbed onto a HOPG electrode under applied potential. Synthetic oligodeoxynucleotides (ODNs) are ideal chemical recognition elements in a DNA biosensor for hybridization detection because the hybridization is highly sequence-selective, and they provide an electrochemical signal due to the oxidation of guanosine and adenosine residues.

To elucidate the mechanism of binding of the short ODN molecules on carbon electrode surfaces, free adsorption and electrochemical

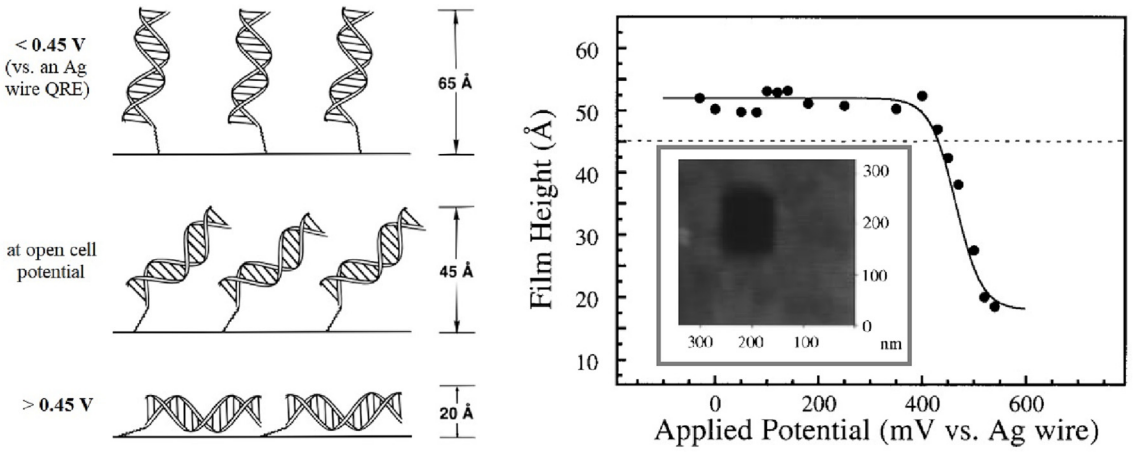

Fig. 2. DNA helices on gold under electrical potential: Left: DNA orientation. Right: DNA monolayer thickness depends on applied potential measured by AFM (with Si_3N_4 cantilevers (spring constant: 0.06 N/m) and oxide-sharpened Si_3N_4 probe tips. All images captured for height-contrast analysis were recorded at minimum vertical tip forces of ~200 pN) under electrochemical control (The dashed line corresponds to the open-circuit value. Right insertion: AFM image of DNA-modified gold after mechanical removal of a small square area (~100 nm × 100 nm) of the monolayer. Adapted from Ref. [59] with permission.

deposition were carried out at applied potentials of +0.30 and +0.65 V vs. Ag wire QRE [66].

For ODN samples prepared by free adsorption, ODN solutions were deposited onto freshly cleaved HOPG surfaces and incubated for 3 min at a range of concentrations from 0.1, 0.3 and 0.8 μM. The excess ODN was gently cleaned with a jet of Millipore Milli-Q water, and the HOPG with adsorbed ODNs was then dried with nitrogen.

For ODN samples prepared by electrochemical deposition, 500 μL of ODN solution at a concentration of 0.1, 0.3 and 0.8 μM was placed in the electrochemical cell holding the HOPG working electrode on the base. Positive potentials of 0.30 and 0.65 V vs. AgQRE were applied to the electrode for 3 min. The HOPG with adsorbed ODNs was rinsed with a jet of Millipore Milli-Qwater and dried with nitrogen.

AFM imaging revealed that:

- Free adsorption from a small concentration of 0.1 μM showed that the ODN molecules adsorb spontaneously onto HOPG.
- The small single-stranded 10-mer ODN molecules appear in the AFM images as small globular aggregates, with the measured full width at a half-maximum height varying between 10 and 30 nm.
- Due to the convolution effect of the tip radius, the ODN diameter and length are overestimated in the AFM images.
- The effect of the + 0.30 V vs. AgQRE applied potential on the adsorption and stability of the ODN layer onto HOPG:
  - The degree of HOPG surface coverage with ODN molecules was similar to free adsorption. However, the greater height of the molecules suggests that the ODNs were DNA "denaturated" less on the surface due to electrostatic interaction with the HOPG surface.
- The effect of the + 0.65 V vs. AgQRE, applied potential
  - The monolayer films height obtained at + 0.65 V were smaller than the height of the ODNs adsorbed at + 0.30 V
  - Large-scale AFM images revealed changes in the orientation of the ODN adsorbed layer near HOPG surface defects
  - The adsorbed adjacent domains were oriented at 60° and 120° to each other (as shown on Fig. 3, Right).

These results correlate with work on the AFM investigation of the impact of positive electrical potential on DNA layer morphology [59] (in particular, on decreasing the DNA monolayer height). In addition, they also demonstrate the influence of the electrode-substrate structure on the spatial localization of nucleic acids (see Fig. 3, Right).

3.1.2.2. AFM characterization of ss- and dsDNA on HOPG by adsorption with applied potential at pH 5.3 and 7.0. AFM-based investigation of the influence of applied potential and pH on the morphology of adsorbed DNA on electrode surfaces is described in Ref. [61]. DNA samples were prepared under an applied potential of +0.3 V (vs. Ag wire) for 3 min, placing 500 μL of ssDNA and dsDNA solutions of different concentrations (5 and 60 μg/ml) in the electrochemical cell, holding the HOPG working electrode on the bottom. The HOPG with adsorbed DNA was rinsed with a jet of Millipore Milli Q water and dried with nitrogen.

It should be noted that at potential of +0.3 V (vs. AgQRE) the oxidation of DNA components did not occur. The oxidation potentials of DNA's bases at carbon electrodes (vs. Ag/AgCl, 3 M KCl), at pH = 7.4 (Ref. [67]) are as follows. Guanine (G) base presents Ep ~ +0.70 V; adenine (A) at Ep ~ +0.96 V; thymine (T) at Ep ~ +1.16 V; cytosine (C) at Ep ~ +1.31 V.

It is also necessary to take into account that in the case of using thiolated DNA monolayers, their electrochemical stability is limited to the potential window of −0.6 to +0.6 V, the thiolated DNA being totally stripped off the electrode (the reductive desorption) at −1.3 V versus Ag/AgCl and pH 7 [68].

AFM imaging obtained at different pHs applying a potential of +0.3 V reveal that:

- The dsDNA film was robust enough to withstand the application of high AFM forces without being removed from the surface.
- The DNA adsorbability on the positively charged hydrophobic surface of HOPG electrode increases at pH 5.3 acetate buffer, due to the dsDNA protonation, which increases their hydrophobicity. (Fig. 4, A).
- The DNA adsorbability on the HOPG electrode decreases at physiological pH as the dsDNA phosphate groups are entirely or quasi-fully ionized (deprotonated), which increases their hydrophilicity to almost 100%.
- ssDNA interacts and adsorbs much more strongly to the HOPG surface when compared with dsDNA for the same solution concentration. It's because the bases in ssDNA are more exposed to the solution, which facilitates the interaction of the hydrophobic aromatic rings of the purines and pyrimidines with the hydrophobic HOPG surface.
- The dsDNA adsorbed under an applied potential of + 0.3 V (vs. Ag wire) is much stronger than at the open circuit potential and led to the formation of bigger network holes and a more condensed and compact self-assembled DNA lattice (Fig. 4, C, D).

The presence of pores in the DNA layer (as seen in Fig. 4) opens access to the HOPG surface, which can cause non-specific adsorption and lead to misleading results when using a DNA-electrochemical biosensor to detect hybridization or DNA-drug interactions. Thus, full coverage of the electrode is desirable to minimize such non-specific adsorption. To obtain a denser layer of DNA, it is necessary to increase the concentration of DNA. It, in turn, induces the formation of more than one DNA monolayer and can cause steric hindrance in the

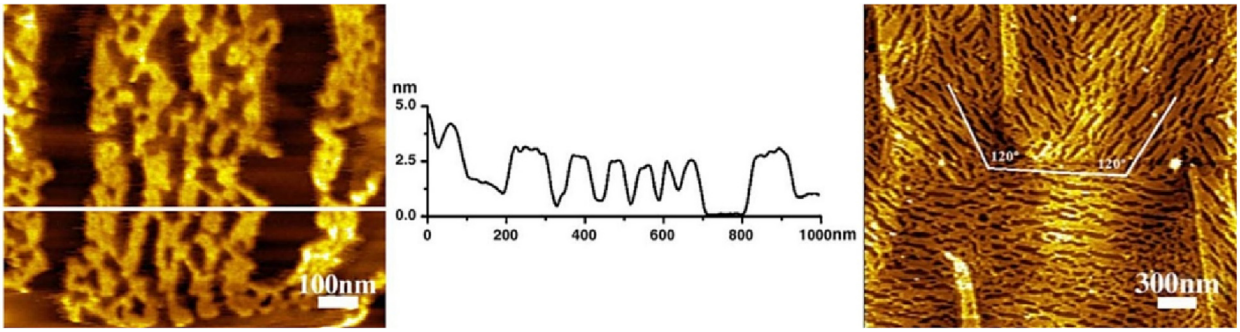

Fig. 3. MAC Mode AFM topographical images of ODN molecules in the air, immobilized on the HOPG surface by adsorption during 3 min, at + 0.65 V vs. AgQRE applied potential, from 0.8 μM ODN in pH 4.5 0.1 M acetate buffer solution. (on the Left and Right). Cross-section profile through white line in the image (Middle). Adapted from Ref. [66] with permission.

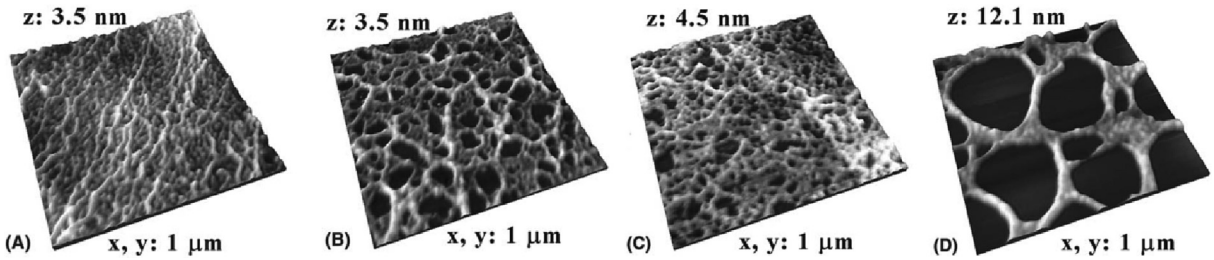

Fig. 4. MAC mode AFM topographical images of DNA molecules immobilized onto HOPG after 3 min in 60 μg/mL dsDNA; (A, B) free adsorption in (A) pH 5.3, 0.1 M acetate buffer and (B) pH 7.0, 0.1 M phosphate buffer; (C, D) at a deposition potential of + 0.3 V (vs. AgQRE) in (C) pH 5.3 0.1 M acetate buffer and (D) pH 7.0 0.1 M phosphate buffer (From Ref. [61] with permission).

hybridization process. It should be mentioned that surface hybridization is the fundamental phenomenon required to use DNA as a recognition element; it involves a target single-stranded DNA (ssDNA) engaging in specific interactions (hybridization) with immobilized probe ssDNA molecules [69]. For effective hybridization, finding a compromise between full surface coverage with DNA and providing enough separation between molecules is necessary.

Taking the above conclusions into account, new questions arise:

- To what extent does surface presence of pore influence the transduction event?
- How density of ssDNA strands on the sensing surface affect hybridization of two complementary strands?

To answer these questions, performing AFM hybridization studies at the single-molecular level is advisable.

3.2. AFM single molecule imaging of hybridization in electrochemical sensors

Joseph et al. [70] observed the nanoscale conformations of individual DNA molecules on a gold surface passivated with a hydroxyl-terminated alkanethiol SAM using in situ electrochemical AFM. Although the visualization of the hybridization process was not performed in this work, the possibility of single-molecule AFM visualization of DNA on an electrode under certain conditions was demonstrated. Moreover, this study clarifies several outstanding questions concerning the switching dynamics of the DNA molecules in response to an applied potential in thiolated DNA monolayers on the gold surface. The results provide evidence that:

- Imaging individual DNA molecules tethered to sensor surfaces under aqueous solutions is complicated by the significant mobility of the molecules.
- DNA can only be imaged when in a "strongly adsorbed" state A (see Fig. 5), which is possibly a result of hydrophobic interactions between the grooves of the DNA and the alkanethiol defect sites, appears as the taller/globular features with the AFM.
- DNA was not clearly resolved by AFM until a potential of + 0.6 V was first applied.
- AFM images of rapidly equilibrated states W* have amorphous features (see Fig. 5).
- The transition to the mobile state is slow on the time scale of the sweep. This is in contrast to fluorescence spectroscopy studies showing that tethered DNA switched within milliseconds between a surface-bound state and a lifted state.
- The 6-mercapto-1-hexanol self-assembled monolayers (SAM) cannot be treated as a static surface, as commonly assumed. The SAM may be actively molded by the DNA at certain potentials.

Thus, taking into account the above mentioned results, it can be concluded that AFM visualization of the hybridization process at the nanoscale level with high resolution is hindered by the presence of contradictions:

- The requirement for high AFM resolution is the immobilization of the molecule (DNA) at the moment when the AFM probe passes over it;

A condition (one of the conditions) for ensuring the possibility of hybridization on the surface is the presence of a passivation layer of

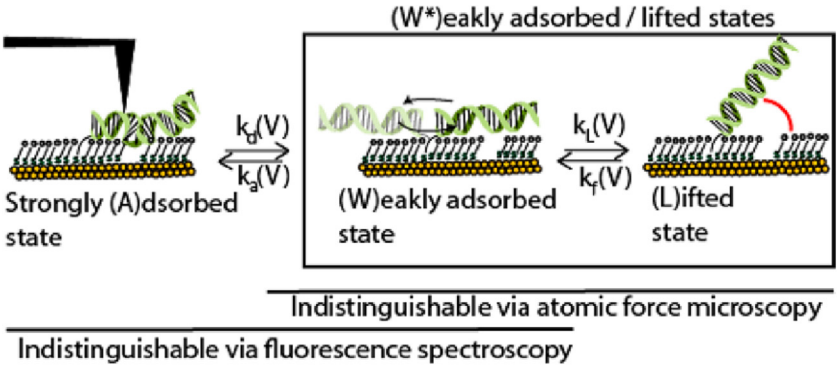

Fig. 5. States of thiolated 105 bp DNA covalently attached to an Au(1 1 1) electrode atop an alkanethiol monolayer. A "strongly adsorbed" state (A), weakly adsorbed state (W), lifted state (L), the rapidly equilibrated states W*. Adapted from Ref. [70] with permission.

inert molecules on the electrode. Non-specific interactions of the DNA and the electrode must be minimized. Due to the presence of a passivated surface, the DNA probes fixed on it retain their dynamic behavior.

Thus, during hybridization, the condition to ensure the immobility of the molecule is not met, so most AFM studies rely on contrast changes of DNA bundles on surfaces, and individual molecules are not recognized (in most early studies).

In a follow-up study, the same group demonstrated that the hybridization of individual DNA molecules could be visualized on carboxyl-terminated SAMs on the gold surface with an unprecedented lateral resolution (~3 nm) using AFM [71].

Since the carboxyl end groups are ionized at pH 8.0 and have a negative charge, it is expected that the probes will rise above the surface due to the electrostatic repulsion of the DNA. The electrostatic repulsion by the surface, confined to within a few Debye lengths (0.3 nm), is not expected to hinder hybridization significantly. Thus, during the short-term repulsive interaction of the surface with DNA, hybridization was carried out, while AFM imaging took place in the presence of Ni^{2+}, which ensured the adsorption of DNA on the surface. As a result, the use of AFM for high-resolution imaging of single DNA hybridization events was achieved by switching the DNA-surface interaction between a strong and weak state (see Fig. 6).

These results highlight that AFM enabled spatial resolution of single DNA molecules that are tethered to SAMs on gold. However, this work does not assess the spatial heterogeneity of the system, as the kinetics of surface hybridization was characterized using the overall hybridization yield.

In more recent studies, Gu et al. [72] have investigated for the first time how the spatial patterns of single DNA probe molecules impact the surface DNA hybridization on an electrochemical biosensor. For this purpose, they have developed a model surface of a DNA probe tethered to highly ordered SAMs with an inter-probe separation of less than 10 nm (Fig. 5). (for probe density 5×10^{12} or 1×10^{13} /cm^2 many of the molecules are separated by less than 10 nm) [48] Such a platform minimizes the impact of uncontrolled morphological and compositional heterogeneities. This allows investigation of how the spatial organization of single molecules alters molecular recognition. The 11-mercaptoundecanoic acid (MUDA) SAM on single-crystal Au (1 1 1) disk electrodes was exposed to solutions containing different concentrations of thiolated DNA probes, ranging from 100 nM to 4 μM. When the concentration is 4 μM, the resulting immobilized individual probe molecules are difficult to resolve due to significant overlap between the molecular features. Hence only a lower limit, 2×10^{12} probes/cm^2 could be estimated. These values cover most of the range of probe surface densities of biosensors and microarrays used in practice, except for the high end, 10^{12} –10^{13} probes/cm^2. While single molecule imaging can directly quantify the probe densities, they also utilized the unique ability to characterize the spatial patterns of single molecules (e.g., spatial heterogeneities), which are inaccessible with existing averaging techniques, using statistical tools, including Ripley's K function [73], nearest-neighbor distances, and local crowding indices. The clustering of target capture suggests that hybridization may be enhanced by the proximity of probes and targets about 10 nm away. The complex interplay between the nanoscale spatial organization of the probe molecules and the conformational changes of the probe molecules rationalized the unexpected enhancement and target binding.

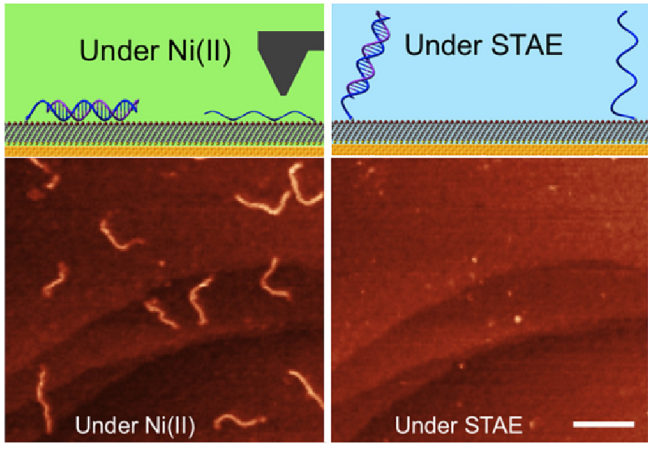

Fig. 6. Schematic and AFM images: Left. Captured dsDNA targets under a buffer containing Ni^{2+}. Right: Image of the same area after switching to a saline Tris-acetate-EDTA (STAE) buffer. The scale bar is 100 nm. AFM Images: in tapping mode under liquid, silicon tips mounted on silicon nitride cantilevers with a nominal spring constant of 0.3 N/m and a resonant frequency of ~ 16 kHz in liquid (model SNL-10, manufactured by Bruker, California). Adapted from Ref. [71] with permission.

Single-molecule AFM imaging of the hybridization complex (dsDNA) and ssDNA at the sensor surface was acquired to quantify the overall hybridization yield directly. Moreover, from differential pulse voltammetry (DPV) measurement alone, it is unclear whether the incomplete signal suppression is caused by the finite electron transfer rate or incomplete hybridization (Fig. 7, e). Single-molecule AFM analysis allowed for establishing which fraction of DNA probe molecules is inactive. The absence of changes in hybridization yield in response to increasing target concentration allows concluding that the incomplete suppression of the DPV is due to incomplete hybridization.

Moreover, it was concluded that even under a relatively uniform probe density, the remaining distribution of inter-probe distances arising from random probe immobilization may lead to heterogeneous target binding. Therefore, a direct, quantitative correlation between the nanoscale lateral organization of the DNA probes and the overall hybridization kinetics has remained elusive.

To investigate how the interfacial environment influences the overall kinetics of surface hybridization, Gu et al. [74] used similar AFM imaging conditions for high-resolution visualization of the DNA probes and hybridized DNA target molecules in combination with statistical models of single molecule rate constants. It was found that the hybridization kinetics has a non-monotonic trend if the probe density is from 1.83×10^{10} to 2.03×10^{11} probes/cm^2, which is difficult to explain using averaged overall surface densities. However, by examining the local probe spatial organization, such as nearest neighbor distance, which is the nanoscale distance to the closest DNA probe, the trend could be readily explained.

The approach proposed in this work can be a starting point for studying the influence of additional factors, such as the effect of clustering of target molecules and different lengths of probes and targets.

Future studies using in situ electrochemical AFM imaging at a single molecular resolution will help to elucidate the role of background SAM, ionic solution strength, and assembly conditions in guiding the spatial organization and conformations of DNA on surfaces. Resolving DNA conformation dynamics, e.g., during hybridization, presents an additional challenge because AFM scanning may need to be faster to determine the dynamic processes and be coupled with an electrochemical cell.

Thus, this highlight the importance of future experiments, such as the application of high-speed AFM, which should enable additional insights into the orientational switching mechanism at the nanoscale.

Successful imaging of DNA dynamics requires the ability of the system to move over the AFM substrate. At the same time, the sample should remain bound within the scanning area during imaging. Finding appropriate experimental conditions related to the sample preparation procedure and choosing the proper value of electrical potential can accommodate these conflicting conditions.

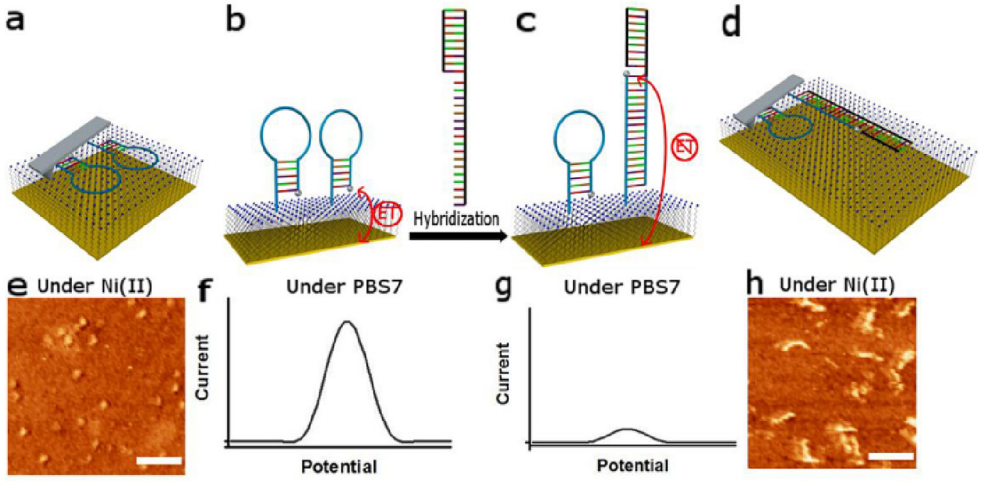

Fig. 7. Schematic of a dynamically switchable E-DNA sensor surface, (a) A stem-loop DNA probe is covalently tethered at one end to a single crystal Au electrode passivated with a MUDA monolayer and modified with a MB tag (Silver) at the other end. The probe is pinned down to the surface after adding Ni^{2+} and thus can be imaged by AFM. (b) After imaging, the surface is rinsed with an STAE buffer and a DPV measurement is carried out under a PBS7 buffer, (c) Upon the addition of a complementary target DNA into the PBS7 buffer, the same DPV measurement is repeated, (d) The hybridized surface is imaged following the same procedure as given in step (a) above. AFM images and DPV signals of the sensor surface (e,f) before and (h,g) after the hybridization with the targets. The scale bar is 25 nm. AFM images were obtained using SNL-10 cantilevers (spring constants of 0.2–0.4 N/m, Bruker, Bellerica, MA, USA) under a Ni^{2+} buffer. Intermittent contact mode AFM imaging with a resonant frequency of approximately 16 kHz was performed. Adapted from Ref. [72] with permission.

3.3. AFM-based single-molecule force spectroscopy with potentiostatic control

The ability to control the interaction of polyelectrolytes, such as DNA, with polarized surfaces is of pivotal importance for a multitude of biotechnological applications. Erdmann et al.[10] performed AFM force spectroscopy measurements with dsDNA covalently bound to the AFM tip, and desorbed this dsDNA from a SAM-modified gold electrode under potentiostatic control. The authors showed that positive potentials induced DNA adsorption onto OH-terminated electrodes with desoption forces in form of force plateaus up to 25 pN (at +0.5 V vs. Ag/AgCl), whereas negative potentials suppressed DNA adsorption. In addition, hysteresis between the desorption force and applied voltage suggest memory effects in the electrode on a timescale much slower than the surface recharging. The work by Erdmann et al. [10] gained valuable insights into the potential-dependent interactions between individual DNA molecules and a SAM. Although force spectroscopy mapping, in principle, should provide the spatial distribution of the interactions across the surface, such kind of mapping is relatively slow and is limited by the stochastic adsorption of DNA molecules.

In the future, the development high speed AFM mechanical mapping could reduce the imaging times of the force spectroscopy mapping. Moreover, the application of high pulling rates may reveal non-equilibrium desorption of DNA from the surface, providing further information about the binding kinetics.

Recently, Shao et al. [75] performed a single molecule force spectroscopy study of the interactions between dsDNA and an 1,1′-biferrocenylene (BFD = bis(fulvalene)diiron)-terminated self-assembled monolayer surface, allowing to reversibly change the charge state. It was found that the interaction force between DNA and the surface was correlated to the oxidation state of the BFD groups which was conveniently controlled by the electrochemical potentials (Fig. 8). The work reported that the electroactive SAM produced much stronger interaction forces than its nonelectroactive counterpart.

To explore the range of approaches to electrical control of the desorption force, further studies could investigate (as well as the different possible polymers) the impact of variation in the alkane chain length and end groups of the SAM, and different ion species and concentrations in the solution. Because AFM has high-resolution feedback control and a force measurement system, it is a good candidate for manipulating a DNA strand through nanopores at a speed low enough to identify a single DNA base.

3.4. Example of the manipulation of DNA transport

Solid-state nanopores, which mimic the protein-based nanopores, have emerged as one of the most promising technologies to decode the sequence of DNA nucleobases. The analytical capabilities of a nanopore-based device are achieved by electrophoretically driving molecules in solution through a nano-scale pore [76]. By applying a biasing electric field, a ssDNA can be driven through a nanopore, and different types of nucleotides yield different ionic currents, thereby realizing the precise single nucleotide sensing. Among solid-state nanomaterial-based devices, grapheme [77] and graphene like materials have been widely examined due to their one-atom thickness, high surface area, and interesting structural, electronic, and transport properties [78]. Combining AFM with nanopore technology, Si et al. [81] developed a measuring system using an DNA coated AFM probe tip to control the dynamics of DNA transport through a silicon nitride nanopore. Success capture events of DNA translocation through the nanopore with the translocation rate of ~100 nm/s were detected by measuring the ion current and the force simultaneously.

Thus, direct AFM-based manipulation technology can accelerate the development of third-generation DNA sequencing using nanopore technology.

3.5. 3D-AFM capabilities in visualization of the nucleic acids hydration

Interfacial liquid layers are involved in a wide range of phenomena, including electrochemistry and electrochemiluminescence. Liquids near a solid surface form an interfacial layer present different organization than molecules in the bulk. Water not only acts as a solvent. The hydration of biomolecules influences their structure, dynamics and function. Water molecules are known to interact between DNA and minor-groove binders [79]. (NOTE. Minor groove is the target of a large number of non-covalent binding agents. Binding takes place by means of a combination of directed hydrogen bonding to base pair

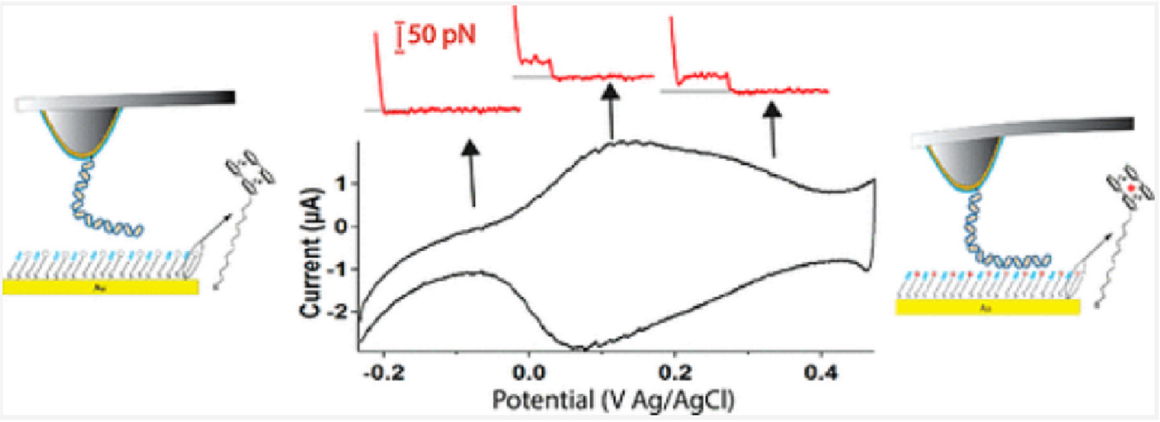

Fig. 8. Single molecule force spectroscopy study and its correlation to the oxidation state of the bis(fulvalene)diiron (BFD) groups, conveniently controlled by the electrochemical potentials. Adapted from Ref. [75] with permission.

edges, van der Waals interactions with the minor groove walls and generalized electrostatic interactions) [80].

The dsDNA is stabilized by a configuration of water molecules bound to its minor groove, aptly known as the "spine of hydration", while competition between water molecules and biomolecules over interaction with DNA is known to steer biological processes [82]. Release of partially ordered water from the hydrated layer upon the binding of interacting partners is a source of entropic force [83]. Structure and molecular dynamics of water in hydrated DNA and RNA have been studied by advanced physical methods [84], such as crystallography [85], high-resolution solid-state NMR spectroscopy [86], osmotic stress [87], and volumetric strategy [88], as well as molecular dynamics simulation. The results showed that electric forces at the DNA surface mainly originate from water molecules in the first two hydration layers and the water-bridge lifetime in the DNA and RNA groove varies from 1 to 300 ps, depending on the sequence.

Currently, 3D-AFM has been applied to measure hydration layers on DNA [89]. Frequency Modulation AFM (***FM-AFM) emerged in recent years as a powerful tool for imaging the interface between solid surfaces and aqueous solutions.*** FM-AFM utilizes a sharp tip located at the edge of a cantilever [90]. The cantilever is oscillated at its resonance frequency, defined by a $\pi/2$ phase-lag of the tip position relative to the driving force. Tip-sample interactions shift the cantilever resonance frequency during scanning, while the $\pi/2$ phase-lag is maintained by a feedback loop. A 3D resonance frequency map is generated by adding another step to the 2D topography scan. The 3D Δf image is constructed from either approaching or retracting Z profiles at each XY positions (Fig. 9). Once the z-loop reaches a set-point frequency at a certain pixel, the z-loop deactivates and the tip scans up and down from that point, generating a frequency shift vs. distance curve. The z-loop then reactivates, and the tip is moved to the next pixel. Finally, one obtains a map where each pixel in a 3D volume above the sample surface is associated with a frequency shift.

For cantilever oscillation amplitudes much smaller than the interaction range, the frequency shift is proportional to the gradient of the total conservative force acting on the tip. Kuchuk et al. [90] successfully demonstrated the use of FM-AFM to generate 3D hydration maps of single DNA molecules under near-physiological conditions (see Fig. 10). These examples illustrate the capabilities of 3D-AFM to provide real-space images of the hydration structure and the local EDL of biomolecules. The spatial distribution of water was identified by plotting the frequency shift of the cantilever resonance as a function of the position in xyz. The regions with higher frequency shifts are indicative of higher values in the density of water molecules.

4. Conclusions and future outlook

In this review, we analyzed the applicability of AFM to the study of the characteristics of DNA on solid–liquid and solid-air conductive surfaces. Early and modern AFM studies in this context were analyzed. It should be noted that although AFM is widely used to characterize functional surfaces, particularly electrochemical biosensors, AFM analysis was often limited to providing morphological images of the surface without analyzing process-structure–property correlations. Herein, we focused exclusively on works that perform process-structure–property correlations. Although there is still a limited number of works in this context, their presence demonstrates the promising applicability of the AFM approach. Such studies require the coupling of electrochemical and AFM equipment, as well as appropriate experience in both directions and (or) collaboration of researchers. The presence of a biological component, such as DNA, on a conductive surface under the action of a potential difference requires additional biological skills. The relatively small number of works in this area is a sign of the intrinsic difficulty of the topic. Therefore, there is plenty of room for further progress of AFM research of bioelectrochemical interfaces at the nanoscale level under electrochemical control in the investigation of "structure–property," "process-structure," and "process-structure–property" correlations.

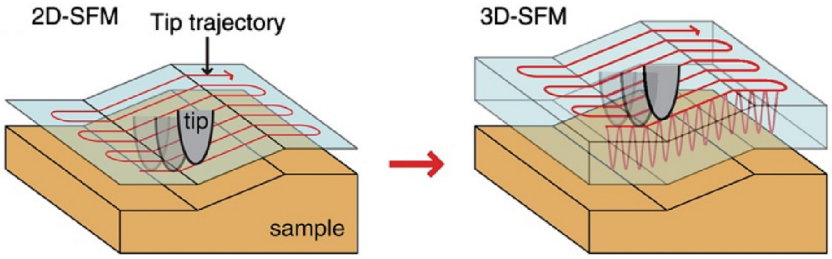

Fig. 9. Basic principles of 3D- Scanning force microscopy (SFM) vs. 2D- (SFM). Adapted from Ref. [90] with permission.

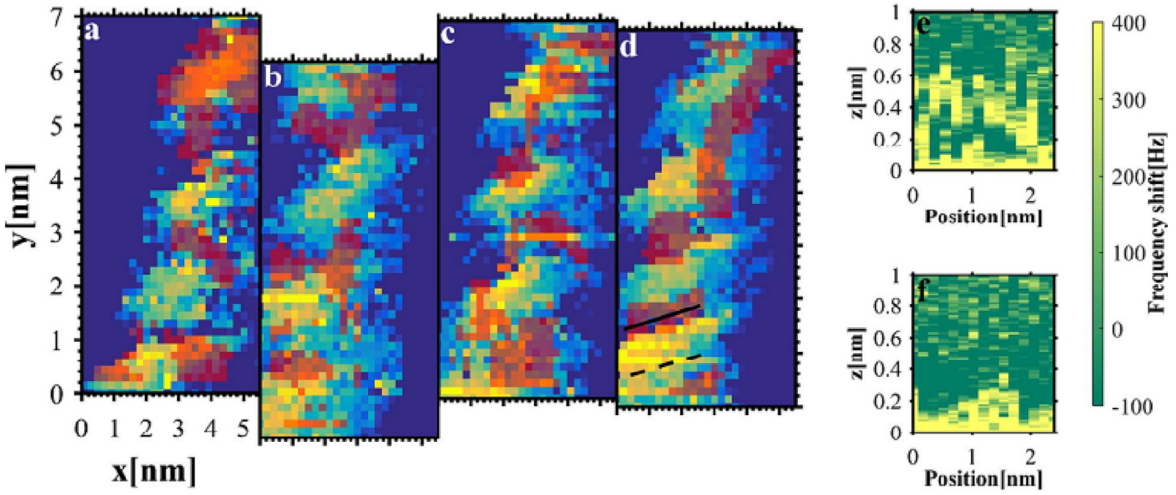

Fig. 10. (a-d) Hydration of the same section of a DNA molecule, measured in four consecutive 3D scans. (b-d) were shifted vertically with respect to (a) to align identical grooves. Pixels shaded red indicate high hydration density. Shaded pixels located to the sides of the molecule (dark blue region) have been removed for clarity. (e) Cross-section of frequency shift data along the solid line in (d) that passes through a hydrated domain in the groove showing clear hydration oscillations. (f) Cross-section of frequency shift data along the dashed line in (d) that passes through the sugar-phosphate backbone and does not show hydration oscillations. Adapted from Ref. [91] with permission. (For interpretation of the references to colour in this figure legend, the reader is referred to the web version of this article.)

In our opinion, the following issues will contribute to the advancement of the field:

i. Combining methods of analysis from electrochemistry and biological AFM at the methodological, hardware, and software levels.
ii. Overcoming scientific and instrumental challenges related to *imaging speed*.

The acquisition time of an image should be fast enough to track the dynamic events, such as DNA conformation in response of electric field, interaction with different conductive solid surfaces, etc. This time should be reduced significantly, for example, by using technologies developed for high-speed AFM imaging.

iii. In post-processing of AFM data
- using mathematical models that are able, for example, to scale-up the data obtained on nano-micrometer areas (in particular, this is relevant for finding an answer to the question of how heterogeneity in local areas affects the electrochemical signal, which is an integral characteristic of the sensor surface).
- the use of computer chemistry equipment (molecular dynamics, molecular mechanics, molecular docking, etc.) to verify and facilitate the interpretation of experimental research results.,
- use of artificial intelligence for data and image analysis.

Summing up, synergism is the short answer to the question posed in the title of this review. Thus, the use of AFM for studying DNA on conducting surfaces, including in the presence of a potential difference, may go beyond the scope of a tool for characterizing the surfaces of electrochemical (bio)sensors. And the degree of expansion of these boundaries will be determined by the art of applying a multidisciplinary approach where the total effect becomes more than the sum of the individual approaches.

Consideration

Prof. Erkang Wang receives the authors' heartfelt congratulations on his 90th birthday. The authors are incredibly grateful for the opportunity to meet him in person. His eyes light up with scientific enthusiasm, igniting our desire to conduct R&D.

CRediT authorship contribution statement

Kateryna Muzyka: Conceptualization, Writing - review & editing. **Felix Rico:** Writing - review & editing. **Guobao Xu:** Writing - review & editing. **Ignacio Casuso:** Conceptualization, Writing - review & editing.

Data availability

The authors do not have permission to share data.

Declaration of Competing Interest

The authors declare the following financial interests/personal relationships which may be considered as potential competing interests: Kateryna Muzyka, Ignacio Casuso reports financial support was provided by French National Research Agency.

Acknowledgements

This work was supported by the French National Research Agency (ANR-21-CE42-0031) and Pause Programme (France) (application #2022000142).

References

[1] E.E. Ferapontova, Electron Transfer in DNA at Electrified Interfaces, Chemistry 14 (21) (2019) 3773–3781.
[2] D. Porath, G. Cuniberti, R. Di Felice, Charge Transport in DNA-Based Devices, in: Long-Range Charge Transfer in DNA II, Schuster, G. B., Ed. Springer Berlin Heidelberg, Berlin, Heidelberg, 2004; pp 183–228.
[3] D. Ho, W. Hetrick, N. Le, A. Chin, R.M. West, Editors' Choice—Electric Field-Induced DNA Melting with Detection by Square Wave Voltammetry, J. Electrochem. Soc. 166 (4) (2019) B236.
[4] P. Mali, N. Bhattacharjee, P.C. Searson, Electrochemically Programmed Release of Biomolecules and Nanoparticles, Nano Lett. 6 (6) (2006) 1250–1253.
[5] S. Takeishi, U. Rant, T. Fujiwara, K. Buchholz, T. Usuki, K. Arinaga, K. Takemoto, Y. Yamaguchi, M. Tornow, S. Fujita, G. Abstreiter, N. Yokoyama, Observation of electrostatically released DNA from gold electrodes with controlled threshold voltages, J. Chem. Phys. 120 (12) (2004) 5501–5504.

[6] M. Masi, P. Bollella, E. Katz, Biomolecular Release Stimulated by Electrochemical Signals at a Very Small Potential Applied, Electroanalysis 32 (1) (2020) 95–103.
[7] X. Zhao, Y. Li, R. Sun, Y. Fan, X. Mu, Y. Wang, C. Shi, C. Ma, Electrical potential-assisted DNA-RNA hybridization for rapid microRNA extraction, Anal. Bioanal. Chem. 414 (11) (2022) 3529–3539.
[8] R.M. West, Review—Electrical Manipulation of DNA Self-Assembled Monolayers: Electrochemical Melting of Surface-Bound DNA, J. Electrochem. Soc. 167 (3) (2020) 037544.
[9] A.M. Chiorcea-Paquim, A.M. Oliveira-Brett, DNA Electrochemical Biosensors for In Situ Probing of Pharmaceutical Drug Oxidative DNA Damage, Sensors (Basel) 21 (4) (2021) 1125–1150.
[10] M. Erdmann, R. David, A. Fornof, H.E. Gaub, Electrically controlled DNA adhesion, Nat. Nanotechnol. 5 (2) (2010) 154–159.
[11] E.E. Ferapontova, DNA Electrochemistry and Electrochemical Sensors for Nucleic Acids, Annu. Rev. Anal. Chem. 11 (1) (2018) 197–218.
[12] K. Muzyka, M. Saqib, Z. Liu, W. Zhang, G. Xu, Progress and challenges in electrochemiluminescent aptasensors, Biosens. Bioelectron. 92 (2017) 241–258.
[13] Z. Ning, M. Chen, G. Wu, Y. Zhang, Y. Shen, Recent advances of functional nucleic acids-based electrochemiluminescent sensing, Biosens. Bioelectron. 191 (2021) 113462.
[14] N. Asefifeyzabadi, P.K. Das, A.H. Onorimuo, G. Durocher, M.H. Shamsi, DNA interfaces with dimensional materials for biomedical applications, RSC Adv. 11 (45) (2021) 28332–28341.
[15] K.G.G. Pattiya Arachchillage, S. Chandra, A. Piso, T. Qattan, J.M. Artes Vivancos, RNA BioMolecular Electronics: towards new tools for biophysics and biomedicine, J. Mater. Chem. B 9 (35) (2021) 6994–7006.
[16] A. Sarkar, Biosensing, Characterization of Biosensors, and Improved Drug Delivery Approaches Using Atomic Force Microscopy: A Review, Front. Nanotechnol. 3 (2022) 798928.
[17] Y. Kim, W. Kim, J.W. Park, Principles and Applications of Force Spectroscopy Using Atomic Force Microscopy, Bull. Kor. Chem. Soc. 37 (12) (2016) 1895–1907.
[18] I. Casuso, L. Redondo-Morata, F. Rico, Biological physics by high-speed atomic force microscopy, Philos. Trans. R. Soc. A Math. Phys. Eng. Sci. 378 (2186) (2020) 20190604.
[19] H.G. Hansma, Surface biology of DNA by atomic force microscopy, Annu. Rev. Phys. Chem. 52 (1) (2001) 71–92.
[20] K.H.S. Main, J.I. Provan, P.J. Haynes, Atomic force microscopy-A tool for structural and translational DNA research, APL Bioeng. 5 (3) (2021) 031504.
[21] A.J. Lee, M. Szymonik, J.K. Hobbs, C. Wälti, Tuning the translational freedom of DNA for high speed AFM, Nano Res. 8 (6) (2015) 1811–1821.
[22] J. Hu, M. Wang, H.U.G. Weier, P. Frantz, W. Kolbe, D.F. Ogletree, M. Salmeron, Imaging of Single Extended DNA Molecules on Flat (Aminopropyl)triethoxysilane −Mica by Atomic Force Microscopy, Langmuir 12 (7) (1996) 1697–1700.
[23] Z. Liu, Z. Li, H. Zhou, G. Wei, Y. Song, L. Wang, Imaging DNA molecules on mica surface by atomic force microscopy in air and in liquid, Microsc. Res. Tech. 66 (4) (2005) 179–185.
[24] H.G. Hansma, D.E. Laney, M. Bezanilla, R.L. Sinsheimer, P.K. Hansma, Applications for atomic force microscopy of DNA, Biophys. J. 68 (5) (1995) 1672–1677.
[25] S.C. Oliveira, A.M. Oliveira-Brett, DNA-electrochemical biosensors: AFM surface characterisation and application to detection of in situ oxidative damage to DNA, Comb. Chem. High Throughput Screen. 13 (7) (2010) 628–640.
[26] E.A. Josephs, T. Ye, A Single-Molecule View of Conformational Switching of DNA Tethered to a Gold Electrode, J. Am. Chem. Soc. 134 (24) (2012) 10021–10030.
[27] K.W. Shinato, F. Huang, Y. Jin, Principle and application of atomic force microscopy (AFM) for nanoscale investigation of metal corrosion, Corros. Rev. 38 (5) (2020) 423–432.
[28] T. Ando, High-speed atomic force microscopy and its future prospects, Biophys. Rev. 10 (2) (2018) 285–292.
[29] K.C. Neuman, A. Nagy, Single-molecule force spectroscopy: optical tweezers, magnetic tweezers and atomic force microscopy, Nat. Methods 5 (6) (2008) 491–505.
[30] F. Sumbul, F. Rico, Single-Molecule Force Spectroscopy: Experiments, Analysis, and Simulations, in: Atomic Force Microscopy: Methods and Protocols, Santos, N. C.; Carvalho, F. A., Eds. Springer New York: New York, NY, 2019; pp 163-189.
[31] H. Chen, Z. Qin, M. He, Y. Liu, Z. Wu, Application of Electrochemical Atomic Force Microscopy (EC-AFM) in the Corrosion Study of Metallic Materials, Materials 13 (3) (2020) 668.
[32] Y. Gan, Atomic and subnanometer resolution in ambient conditions by atomic force microscopy, Surf. Sci. Rep. 64 (3) (2009) 99–121.
[33] N. Gadegaard, Atomic force microscopy in biology: technology and techniques, Biotech. Histochem. 81 (2–3) (2006) 87–97.
[34] N. Jalili, K. Laxminarayana, A review of atomic force microscopy imaging systems: application to molecular metrology and biological sciences, Mechatronics 14 (8) (2004) 907–945.
[35] R. Garcı´a, R. Pérez, Dynamic atomic force microscopy methods, Surf. Sci. Rep. 47 (6) (2002) 197–301.
[36] D. Alsteens, H.E. Gaub, R. Newton, M. Pfreundschuh, C. Gerber, D.J. Müller, Atomic force microscopy-based characterization and design of biointerfaces, Nat. Rev. Mater. 2 (5) (2017) 17008.
[37] F. Eghiaian, F. Rico, A. Colom, I. Casuso, S. Scheuring, High-speed atomic force microscopy: Imaging and force spectroscopy, FEBS Lett. 588 (19) (2014) 3631–3638.
[38] Q. Chang, Chapter 7 - Electrical Properties, in: Colloid and Interface Chemistry for Water Quality Control, Chang, Q., Ed. Academic Press, 2016, pp 79-136.
[39] U. Rant, K. Arinaga, S. Fujita, N. Yokoyama, G. Abstreiter, M. Tornow, Electrical manipulation of oligonucleotides grafted to charged surfaces, Org. Biomol. Chem. 4 (18) (2006) 3448–3455.
[40] U. Rant, K. Arinaga, M. Tornow, Y.W. Kim, R.R. Netz, S. Fujita, N. Yokoyama, G. Abstreiter, Dissimilar Kinetic Behavior of Electrically Manipulated Single- and Double-Stranded DNA Tethered to a Gold Surface, Biophys. J. 90 (10) (2006) 3666–3671.
[41] M. Tornow, K. Arinaga, U. Rant, Electrical Manipulation of DNA on Metal Surfaces, in: O. Shoseyov, I. Levy (Eds.), NanoBioTechnology: BioInspired Devices and Materials of the Future, Humana Press, Totowa, NJ, 2008, pp. 187–214.
[42] W. Kaiser, U. Rant, Conformations of End-Tethered DNA Molecules on Gold Surfaces: Influences of Applied Electric Potential, Electrolyte Screening, and Temperature, J. Am. Chem. Soc. 132 (23) (2010) 7935–7945.
[43] U. Rant, K. Arinaga, S. Fujita, N. Yokoyama, G. Abstreiter, M. Tornow, Dynamic Electrical Switching of DNA Layers on a Metal Surface, Nano Lett. 4 (12) (2004) 2441–2445.
[44] U. Rant, K. Arinaga, S. Scherer, E. Pringsheim, S. Fujita, N. Yokoyama, M. Tornow, G. Abstreiter, Switchable DNA interfaces for the highly sensitive detection of label-free DNA targets, Proc. Natl. Acad. Sci. 104(44) (2007) 17364–17369.
[45] U. Rant, Sensing with electro-switchable biosurfaces, Bioanal. Rev. 4 (2) (2012) 97–114.
[46] M. Gębala, W. Schuhmann, Controlled Orientation of DNA in a Binary SAM as a Key for the Successful Determination of DNA Hybridization by Means of Electrochemical Impedance Spectroscopy, ChemPhysChem 11 (13) (2010) 2887–2895.
[47] P. Gong, R. Levicky, DNA surface hybridization regimes, Proc. Natl. Acad. Sci. U.S. A. 105(14) (2008) 5301–5306.
[48] A.N. Rao, D.W. Grainger, Biophysical properties of nucleic acids at surfaces relevant to microarray performance, Biomater. Sci. 2 (4) (2014) 436–471.
[49] M. Gebala, W. Schuhmann, Understanding properties of electrified interfaces as a prerequisite for label-free DNA hybridization detection, PCCP 14 (43) (2012) 14933–14942.
[50] V. Ortiz, J.J. de Pablo, Molecular origins of DNA flexibility: sequence effects on conformational and mechanical properties, Phys. Rev. Lett. 106 (23) (2011) 238107.
[51] L. Bao, X. Zhang, L. Jin, Z.-J. Tan, Flexibility of nucleic acids: From DNA to RNA*, Chin. Phys. B 25 (1) (2016) 018703.
[52] D. Murugesapillai, S. Bouaziz, L.J. Maher, N.E. Israeloff, C.E. Cameron, M.C. Williams, Accurate nanoscale flexibility measurement of DNA and DNA–protein complexes by atomic force microscopy in liquid, Nanoscale 9 (31) (2017) 11327–11337.
[53] C.G. Baumann, S.B. Smith, V.A. Bloomfield, C. Bustamante, Ionic effects on the elasticity of single DNA molecules, Proc. Natl. Acad. Sci. U.S.A. 94(12) (1997) 6185–6190.
[54] W. Reusch, Nucleic Acids, https://www2.chemistry.msu.edu/faculty/reusch/VirtTxtJml/nucacids.htm 2022.
[55] J. Bonnet, M. Colotte, D. Coudy, V. Couallier, J. Portier, B. Morin, S. Tuffet, Chain and conformation stability of solid-state DNA: implications for room temperature storage, Nucl. Acids Res. 38 (5) (2010) 1531–1546.
[56] S. Ayala-Torres, Y. Chen, T. Svoboda, J. Rosenblatt, B. Van Houten, Analysis of gene-specific DNA damage and repair using quantitative polymerase chain reaction, Methods (San Diego, Calif.) 22 (2) (2000) 135–147.
[57] V. Gabelica, E.D. Pauw, Comparison between solution-phase stability and gas-phase kinetic stability of oligodeoxynucleotide duplexes, J. Mass Spectrom. 36 (4) (2001) 397–402.
[58] W.J. Chung, Y. Cui, C.S. Chen, W.H. Wei, R.S. Chang, W.Y. Shu, I.C. Hsu, Freezing shortens the lifetime of DNA molecules under tension, J. Biol. Phys. 43 (4) (2017) 511–524.
[59] S.O. Kelley, J.K. Barton, N.M. Jackson, L.D. McPherson, A.B. Potter, E.M. Spain, M. J. Allen, M.G. Hill, Orienting DNA Helices on Gold Using Applied Electric Fields, Langmuir 14 (24) (1998) 6781–6784.
[60] Z.-L. Zhang, D.-W. Pang, R.-Y. Zhang, J.-W. Yan, B.-W. Mao, Y.-P. Qi, Investigation of DNA Orientation on Gold by EC-STM, Bioconjug. Chem. 13 (1) (2002) 104–109.
[61] A.M. Oliveira Brett, A.-M. Chiorcea, Effect of pH and applied potential on the adsorption of DNA on highly oriented pyrolytic graphite electrodes. Atomic force microscopy surface characterisation, Electrochem. Commun. 5 (2) (2003) 178–183.
[62] A.M. Chiorcea, A.M. Oliveira Brett, Atomic force microscopy characterization of an electrochemical DNA-biosensor, Bioelectrochemistry 63 (1–2) (2004) 229–232.
[63] A.M. Chiorcea Paquim, V.C. Diculescu, T.S. Oretskaya, A.M. Oliveira Brett, AFM and electroanalytical studies of synthetic oligonucleotide hybridization, Biosens. Bioelectron. 20 (5) (2004) 933–944.
[64] A.M. Oliveira Brett, A.M. Chiorcea Paquim, V. Diculescu, T.S. Oretskaya, Synthetic oligonucleotides: AFM characterisation and electroanalytical studies, Bioelectrochemistry 67 (2) (2005) 181–190.
[65] A.M. Oliveira Brett, A.M. Chiorcea Paquim, DNA imaged on a HOPG electrode surface by AFM with controlled potential, Bioelectrochemistry 66 (1–2) (2005) 117–124.
[66] A.-M. Chiorcea Paquim, T.S. Oretskaya, A.M. Oliveira Brett, Atomic force microscopy characterization of synthetic pyrimidinic oligodeoxynucleotides adsorbed onto an HOPG electrode under applied potential, Electrochim. Acta 51 (24) (2006) 5037–5045.
[67] A.M. Oliveira-Brett, J.A.P. Piedade, L.A. Silva, V.C. Diculescu, Voltammetric determination of all DNA nucleotides, Anal. Biochem. 332 (2) (2004) 321–329.
[68] J. Wang, G. Rivas, M. Jiang, X. Zhang, Electrochemically Induced Release of DNA from Gold Ultramicroelectrodes, Langmuir 15 (19) (1999) 6541–6545.

[69] J.I.A. Rashid, N.A. Yusof, The strategies of DNA immobilization and hybridization detection mechanism in the construction of electrochemical DNA sensor: A review, Sens. Bio-Sens. Res. 16 (2017) 19–31.
[70] E.A. Josephs, T. Ye, Electric-Field Dependent Conformations of Single DNA Molecules on a Model Biosensor Surface, Nano Lett. 12 (10) (2012) 5255–5261.
[71] G.R. Abel Jr., E.A. Josephs, N. Luong, T. Ye, A Switchable Surface Enables Visualization of Single DNA Hybridization Events with Atomic Force Microscopy, J. Am. Chem. Soc. 135 (17) (2013) 6399–6402.
[72] Q. Gu, W. Nanney, H.H. Cao, H. Wang, T. Ye, Single Molecule Profiling of Molecular Recognition at a Model Electrochemical Biosensor, J. Am. Chem. Soc. 140 (43) (2018) 14134–14143.
[73] M.A. Kiskowski, J.F. Hancock, A.K. Kenworthy, On the use of Ripley's K-function and its derivatives to analyze domain size, Biophys. J. 97 (4) (2009) 1095–1103.
[74] Q. Gu, H.H. Cao, Y. Zhang, H. Wang, Z.J. Petrek, F. Shi, E.A. Josephs, T. Ye, Toward a Quantitative Relationship between Nanoscale Spatial Organization and Hybridization Kinetics of Surface Immobilized Hairpin DNA Probes, ACS Sens. 6 (2) (2021) 371–379.
[75] J. Shao, R. Breuer, M. Schmittel, T. Ye, Potential-Dependent Adhesion Forces between dsDNA and Electroactive Surfaces, Langmuir 38 (39) (2022) 11899–11908.
[76] D. Branton, D.W. Deamer, A. Marziali, H. Bayley, S.A. Benner, T. Butler, M. Di Ventra, S. Garaj, A. Hibbs, X. Huang, S.B. Jovanovich, P.S. Krstic, S. Lindsay, X.S. Ling, C.H. Mastrangelo, A. Meller, J.S. Oliver, Y.V. Pershin, J.M. Ramsey, R. Riehn, G.V. Soni, V. Tabard-Cossa, M. Wanunu, M. Wiggin, J.A. Schloss, The potential and challenges of nanopore sequencing, Nat. Biotechnol. 26 (10) (2008) 1146–1153.
[77] G.F. Schneider, S.W. Kowalczyk, V.E. Calado, G. Pandraud, H.W. Zandbergen, L.M. K. Vandersypen, C. Dekker, DNA Translocation through Graphene Nanopores, Nano Lett. 10 (8) (2010) 3163–3167.
[78] R.L. Kumawat, B. Pathak, Electronic Conductance and Current Modulation through Graphdiyne Nanopores for DNA Sequencing, ACS Appl. Electron. Mater. 3 (9) (2021) 3835–3845.
[79] B. Nguyen, S. Neidle, W.D. Wilson, A role for water molecules in DNA-ligand minor groove recognition, Acc. Chem. Res. 42 (1) (2009) 11–21.
[80] A. Lauria, A. Montalbano, P. Barraja, G. Dattolo, A.M. Almerico, DNA minor groove binders: an overview on molecular modeling and QSAR approaches, Curr. Med. Chem. 14 (20) (2007) 2136–2160.
[81] W. Si, H. Yang, G. Wu, C. Chen, M. Yu, Manipulation of DNA transport through solid-state nanopores by atomic force microscopy, Mater. Res. Express 7 (9) (2020) 095404.
[82] W. Saenger, W.N. Hunter, O. Kennard, DNA conformation is determined by economics in the hydration of phosphate groups, Nature 324 (6095) (1986) 385–388.
[83] S. Leikin, V.A. Parsegian, D.C. Rau, R.P. Rand, Hydration forces, Annu. Rev. Phys. Chem. 44 (1993) 369–395.
[84] G.I. Likhtenshtein, Nucleic Acids Hydration, in: G.I. Likhtenshtein (Ed.), Biological Water: Physicochemical Aspects, Springer International Publishing, Cham, 2021, pp. 371–405.
[85] M. Egli, P.S. Pallan, Crystallographic Studies of Chemically Modified Nucleic Acids: A Backward Glance, Chem. Biodivers. 7 (1) (2010) 60–89.
[86] S. Zhao, Y. Yang, Y. Zhao, X. Li, Y. Xue, S. Wang, High-resolution solid-state NMR spectroscopy of hydrated non-crystallized RNA, Chem. Commun. 55 (93) (2019) 13991–13994.
[87] E. Rozners, Determination of nucleic acid hydration using osmotic stress, Current protocols in nucleic acid chemistry **2010,** Chapter 7, Unit 7.14. (PubMed Central) doi: 10.1002/0471142700.nc0714s43.
[88] S. Matsumoto, S. Takahashi, S. Bhowmik, T. Ohyama, N. Sugimoto, Volumetric Strategy for Quantitatively Elucidating a Local Hydration Network around a G-Quadruplex, Anal. Chem. 94 (20) (2022) 7400–7407.
[89] T. Fukuma, R. Garcia, Atomic- and Molecular-Resolution Mapping of Solid-Liquid Interfaces by 3D Atomic Force Microscopy, ACS Nano 12 (12) (2018) 11785–11797.
[90] T. Fukuma, Y. Ueda, S. Yoshioka, H. Asakawa, Atomic-scale distribution of water molecules at the mica-water interface visualized by three-dimensional scanning force microscopy, Phys. Rev. Lett. 104 (1) (2010) 016101.
[91] K. Kuchuk, U. Sivan, Hydration Structure of a Single DNA Molecule Revealed by Frequency-Modulation Atomic Force Microscopy, Nano Lett. 18 (4) (2018) 2733–2737.